Peer reviewed and published as received.

a

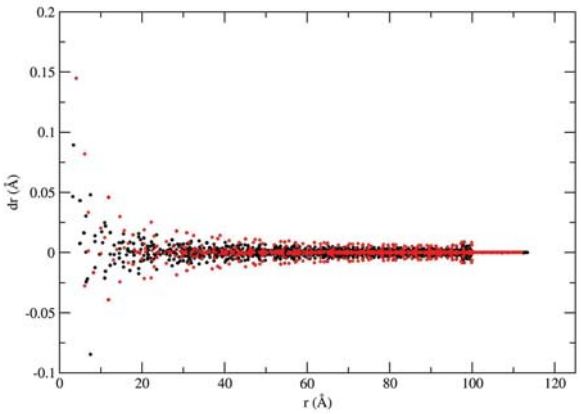

b

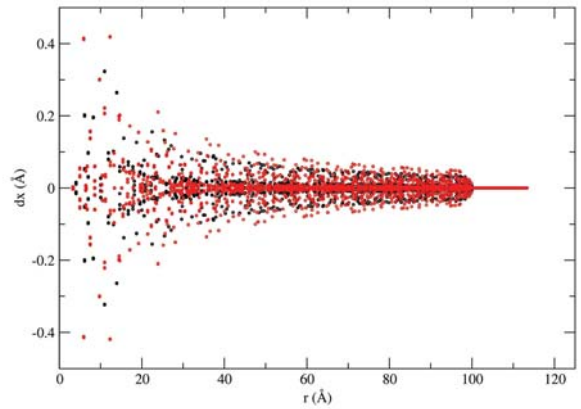

FIGURE S1

Displacements perpendicular to **a**, and along **b**, the dislocation line during atomic relaxation. This represents the difference between the displacement field predicted by linear elasticity and that including core effects. Oxygen cores are in black and silicon atoms are red.

a

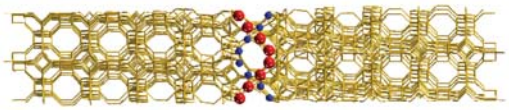

b

FIGURE S2

Two possible screw dislocations in the zeolite A structure viewed perpendicular to the dislocation line. **a**, Shows the **a** <100> dislocation centred on a 8-ring channel, two 8-rings form an interpenetrating double helix shown in red and blue with a pitch of 24 Å. **b**, Shows the $^{1}/_{2}$**a** <100> dislocation where two 8-rings fuse to form a single helix with a 12 Å pitch.

Supporting information

Table S1: Pore dimensions, bond distance and geometry of the 8-rings shown in **Fig. 3**.

	8-ring in bulk (figure 3a)	**8-ring adjacent to dislocation line (figure 3b)**	**Central helix (figure 3c)**
O – O distances across ring (Å)			
1 – 5	6.78	5.95	8.87 (7.85)[a]
2 – 6	6.59	7.36	8.75 (7.99)[a]
3 – 7	6.78	7.85	8.87 (7.85)[a]
4 – 8	6.59	6.88	8.75 (7.99)[a]
Si – Si distances across ring (Å)			
A – E	8.11	7.18	9.81 (6.64)[a]
B – F	8.11	9.34	9.81 (6.64)[a]
C – G	8.11	9.21	9.81 (6.64)[a]
D – H	8.11	7.44	9.81 (6.64)[a]
Si – O bond distances (Å)			
A – 1 and E – 5	1.60	1.70	1.71
A – 2 and E – 6	1.61	1.69	1.70
B – 2 and F – 6	1.61	1.61	1.70
B – 3 and F – 7	1.60	1.57	1.71
C – 3 and G – 7	1.60	1.57	1.71
C – 4 and G – 8	1.61	1.65	1.70
D – 4 and H – 8	1.61	1.63	1.70
D – 5 and H – 1	1.60	1.72	1.71
O – O nearest neighbours (Å)			
1 – 2 and 5 – 6	2.55	3.15	2.90
2 – 3 and 6 – 7	2.55	2.38	2.90
3 – 4 and 7 – 8	2.55	2.32	2.90
4 – 5 and 8 – 1	2.55	2.87	2.90
Si – Si nearest neighbours (Å)			
A – B and E – F	3.08	3.29	3.32
B – C and F – G	3.13	2.99	3.67
C – D and G – H	3.08	3.15	3.32
D – E and H – A	3.13	3.39	3.67
O – Si – O angles (˚)			
1 – A – 2 and 5 – E – 6	104.9	135.1	116.5
2 – B – 3 and 6 – F – 7	104.9	96.3	116.5
3 – C – 4 and 7 – G – 8	104.9	92.1	116.5
4 – D – 5 and 8 – H – 1	104.9	117.4	116.5
Si – O – Si angles (˚)			
A – 1 – H and D – 5 – E	154.9	161.4	159.2
A – 2 – B and E – 6 – F	145.0	167.9	143.2
B – 3 – C and F – 7 – G	154.9	144.9	159.2
C – 4 – D and G – 8 – H	145.0	146.5	143.2

[a] Values in parenthesises have been corrected to allow for pitch of dislocation and give the apparent width of the channel.

Table S2: Potential parameters used for the atomistic model of zeolite A. Functional forms can be found in ref. 36. The values were determined by relaxed fitting to the structure, elastic and dielectric properties of α-quartz.

	Core charge	Shell charge	Spring constant ($eVÅ^{-2}$)	
Si	4	-	-	
O	0.84820	-2.84820	74.9200	
Buckingham potentials	A (eV)	ρ (Å)	C ($eVÅ^6$)	
Si – O	1434.65230	0.312249	10.66000	
O – O	22764.0000	0.149000	27.88000	
Three body exponential potential	k ($eVrad^{-1}$)	θ_0 (°)	ρ_1 ($Å^{-1}$)	ρ_2 ($Å^{-1}$)
O – Si – O	0.862528×10^8	109.4700	0.180000	0.180000

Table S3: Calculated structure and properties for α-quartz, as determined by both the model of Sanders *et al*. (ref 34) and the potential parameters given in Table 2. The experimental data is included for comparison. The percentage deviations of the present model are comparable, if not better, than those of the previous model. Similarly, application of both models to siliceous LTA, where there is no experimental data to compare against, yields almost identical results. The model has also been tested on the low symmetry zeolite silicalite, where it performs comparably with the Sanders *et al.* model and gives excellent agreement with experimental data.

	Experiment	Potential of Sanders *et al*.	Present work
a (Å)	4.9021	4.8707	4.9176
c (Å)	5.3997	5.3778	5.3794
C_{11} (GPa)	86.8	95.3	90.5
C_{33} (GPa)	105.8	112.9	110.6
C_{44} (GPa)	58.2	50.0	46.7
C_{66} (GPa)	39.9	40.4	39.6
ε^{0}_{11}	4.54	4.58	4.22
ε^{0}_{33}	4.64	4.88	4.55
$\varepsilon^{\infty}_{11}$	2.4	2.07	2.01
$\varepsilon^{\infty}_{33}$	2.4	2.09	2.03
υ_{max} (cm^{-1})	1162	1116	1134